Magnetic structures of $PrFeSi_2$ and $NdFeSi_2$ from neutron and Mössbauer studies

B. Malaman and G. Venturini
Laboratoire de Chimie du Solide Minéral, Université de Nancy I, Boîte Postale 239, 54506 Vandoeuvre les Nancy CEDEX, France

G. Le Caër
Laboratoire de Science et Génie des Matériaux Métalliques, Ecole des Mines, 54042 Nancy CEDEX, France

L. Pontonnier and D. Fruchart
Laboratoire de Cristallographie, Centre National de la Recherche Scientifique, 166X, 38042 Grenoble CEDEX, France

K. Tomala* and J. P. Sanchez
Institut de Physique et Chimie des Matériaux et Centre de Recherches Nucléaires de Strasbourg, Boîte Postale 20, 67037 Strasbourg CEDEX, France

(Received 28 July 1989)

Investigations by neutron diffraction and ^{57}Fe Mössbauer measurements are reported on the ternary silicides $RFeSi_2$ (R = Pr, Nd) with the orthorhombic structure of the $TbFeSi_2$-type (space group *Cmcm*). This structure, which is closely related to the $ThCr_2Si_2$-type structure, can be described as isolated $ThCr_2Si_2$ blocks connected via α-$ThSi_2$ slabs. $PrFeSi_2$ orders ferromagnetically below $T_c = 26$ K with magnetic moments [$2.58(1)\mu_B$ at 1.5 K] parallel to the b axis. $NdFeSi_2$ exhibits a more complex magnetic behavior. Below $T_N = 6.5$ K, it develops a sine-modulated antiferromagnetic structure, $\mathbf{q} = (0, 0.591, 0)$, of the Nd moments parallel to the b axis with a maximum value of $2.52\mu_B$ at 4.2 K. No local moment was detected at the iron site. ^{57}Fe Mössbauer data on $NdFeSi_2$ indicate a progressive squaring of the sine modulation of the Nd moments with a pure square wave below 3 K. The comparison of the transferred hyperfine fields at the iron nuclei in $PrFeSi_2$ and $NdFeSi_2$ suggests the occurrence of orbital polarization of the conduction electrons giving rise to anisotropic contributions to the hyperfine field and exchange interactions. The results are discussed in terms of Ruderman-Kittel-Kasuya-Yosida exchange interactions and compared to those obtained previously on the $ThCr_2Si_2$-type ternary silicides.

I. INTRODUCTION

The $RFeSi_2$ silicides (R = La to Nd) crystallize with the $TbFeSi_2$-type structure.[1] The structure is orthorhombic (space group *Cmcm*) and can be described as built of alternating (010) planes containing R, Fe, and Si atoms, respectively, in a RSiFeSiRSiSiRSiFeSi... sequence. Therefore, this structure is closely related to the $ThCr_2Si_2$-type structure (space group $I4/mmm$) (Ref. 2) in which the same atoms lie in alternate layers stacked along the c axis with the sequence ThSiCrSiThSiCrSiTh.... In Fig. 1, we show the blocks which are common to the two structural types. In both cases, the Si atoms form tetrahedra around the transition-metal atoms T and T-Si distances are very short suggesting covalent bonding. On the other hand, these structures exhibit structural relationships with the α-$ThSi_2$-type structure[3] by insertion of transition-metal planes in this structure. α-$ThSi_2$ can be described as $ThSi_8$ tetragonal prisms sharing edges and faces in the (001) planes and stacked along [001] with the following sequence: SiThSi....

A shift ($\mathbf{a}/2$ or $\mathbf{b}/2$) between each adjacent plane yields the formation of Si_4 tetrahedral sites which are filled by the T atoms. We thus obtain the $ThCr_2Si_2$-type structure. When this operation occurs only for half of the planes, we get the $TbFeSi_2$-type structure, which then may be considered as a stacking of both $ThCr_2Si_2$ and α-$ThSi_2$ slabs. Figure 1 clearly shows these structural relationships.

The $TbFeSi_2$ structure can be seen as a still more anisotropic variant of the $ThCr_2Si_2$-type structure. The latter type of compounds has been subject to increased interest for the last few years. This was motivated by the peculiar properties found in some of them, such as superconductivity, Kondo effect, heavy-fermion behavior, valence fluctuation, and magnetism.[4]

Earlier reports on the RFe_2Si_2 series (see Ref. 5 where a large review on the magnetic properties of these compounds can be found) claim that iron atoms have no magnetic moment and only R atoms eventually show antiferromagnetic long range ordering. $NdFe_2Si_2$ was found to order antiferromagnetically below 15.6 K,[6] while $PrFe_2Si_2$ does not exhibit any long-range ordering at 4.2 K.[7]

Hence, studying the magnetic properties of the $RFeSi_2$ compounds appeared to be very interesting. Magnetization measurements on $RFeSi_2$ (R = La to Nd) polycrystalline samples have been still largely described.[8] $LaFeSi_2$

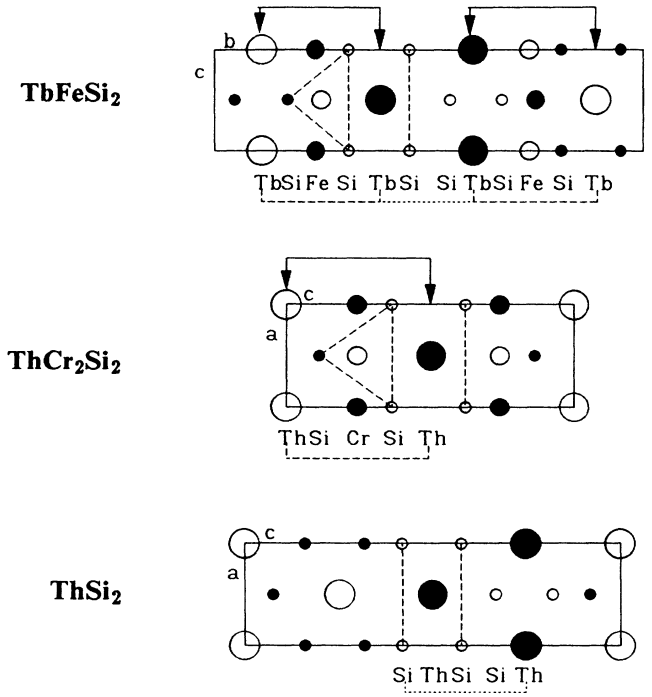

FIG. 1. Structures of $TbFeSi_2$, $ThCr_2Si_2$, and α-$ThSi_2$. Structural relationships.

exhibits a weak Pauli paramagnet behavior, while in $CeFeSi_2$, Ce appears to be in an intermediate valent state. $PrFeSi_2$ is ferromagnetic below 26 K while $NdFeSi_2$ exhibits antiferromagnetic ordering below 6.5 K. In all studied compounds, Fe atoms never carry magnetic moments. The main crystallographic and magnetic data are collected in Table I.

In this paper, we report on extensive study of the magnetic structure of $PrFeSi_2$ and $NdFeSi_2$ compounds, using neutron diffraction and ^{57}Fe Mössbauer spectroscopy. Comparison with the RFe_2Si_2 compounds and a general discussion are given in the conclusion.

II. EXPERIMENTAL PROCEDURES

The RFe_2Si_2 compounds were prepared from commercially available high-purity elements: Fe (powder, 99.9%), rare-earth (R) elements (ingots, 99.9%), and silicon (powder, 99.99%). Pellets of starting composition $RFeSi_2$ (R =Pr,Nd) were compacted using a steel die, and were annealed several times (with grinding and compacting each time) at 1273 K in sealed silica tubes under argon (0.2 atm) and finally quenched in water. Purity of the final samples was determined by an x-ray-diffraction technique using a Guinier camera (Cu $K\alpha$).

Neutron-diffraction experiments were carried out at the Institute Laue-Langevin (ILL), Grenoble. The diffraction patterns were recorded with the one-dimensional curved multidetector D1b at a wavelength λ=2.513 Å. Several patterns were collected in the temperature range 1.5–40 K, namely above and below the ordering temperature for each compound.

The Mössbauer experiments were performed between 1.6 and 295 K at the Institute of Physics and Chemistry of Materials, Strasbourg. Temperatures between 1.6 and 4.2 K were controlled by pumping the helium bath through a manostat. Absorbers of 5 mg Fe/cm^2 were used in order to minimize intensity saturation effects. The source of ^{57}Co/Rh (25 mCi) was moved as a sinusoidal or triangular function of time in synchronization with a multichannel analyzer operating in the time mode. The experimental data were computer analyzed as sums of Lorentzian line shapes according to the proper physical situation.

III. NEUTRON DIFFRACTION

A. Crystal structure determination

The neutron-diffraction pattern recorded in the paramagnetic state is characteristic of only the nuclear scattering (Figs. 2 and 4). The extinction rules of the space group *Cmcm* are fulfilled and confirm unambiguously the $TbFeSi_2$-type structure for $PrFeSi_2$ and $NdFeSi_2$.

TABLE I. $RFeSi_2$ compounds. Main crystallographic and magnetic parameters, Ref. 5.

	Crystallographic data			
Compounds	a (Å)	b (Å)	c (Å)	V (Å^3)
$PrFeSi_2$	4.103(3)	17.04(3)	4.016(3)	281
$NdFeSi_2$	4.082(3)	16.98(3)	4.004(3)	277

		Magnetic data						
compounds	coupling	$T_{C,N}$ (K)	μ at 4.2 K and 150 kG (μ_B)	μ_s [$\mu=f(1/H)$]	gJ (μ_B)	Θ_p (K)	μ_{eff} (μ_B)	$g\sqrt{J(J+1)}$ (μ_B)
$PrFeSi_2$	Ferro.	26	1.88	2.05	3.20	44	3.5	3.58
$NdFeSi_2$	Antiferro.	6.5	1.90[a]	2.22	3.27	41	3.6	3.62

[a]Metamagnetic transition under 24 kG.

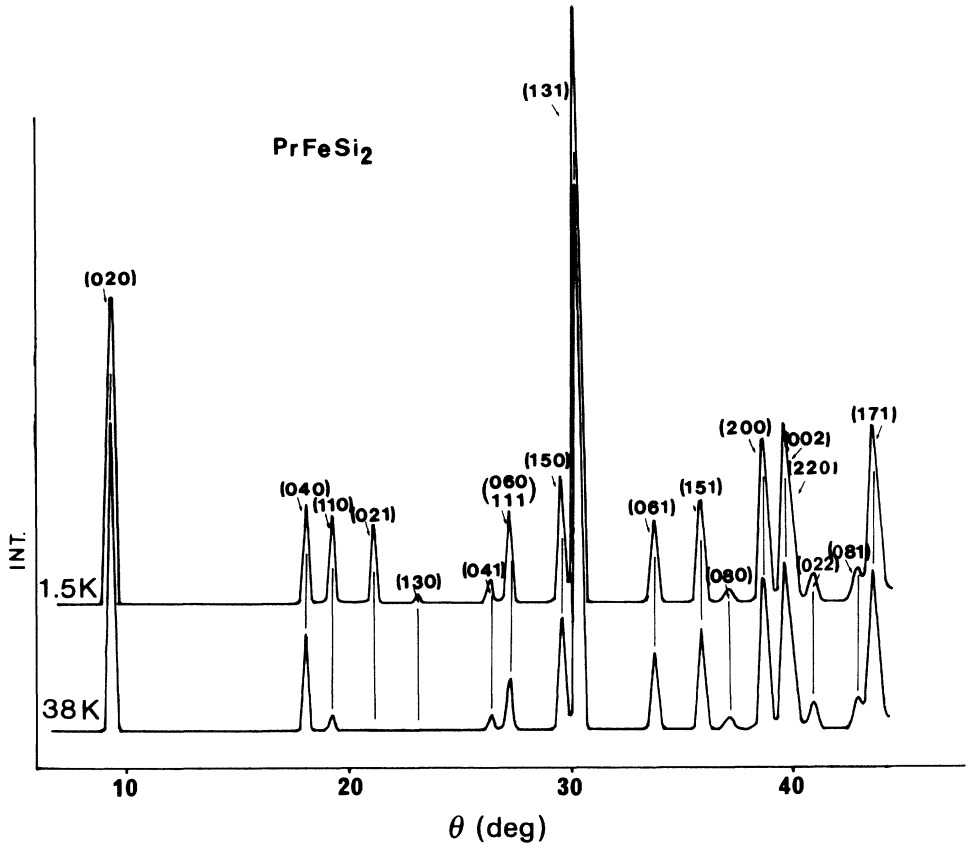

FIG. 2. Neutron-diffraction patterns of $PrFeSi_2$ at 38 and 1.5 K.

Using the scattering lengths $b_{Fe}=9.54$, $b_{Si}=4.152$, $b_{Pr}=4.45$, and $b_{Nd}=7.69$ fermi,[9] the nuclear intensities were calculated using the atomic positions given in Table II.

The scale factor and the atom positions y were refined by a least-squares procedure.[10] Attempts made to fit the nuclear lines by interchanging the position of Fe and Si atoms always led to a poorer agreement and gave no evidence for any mixing between Fe and Si atoms. Furthermore, these results confirm our structural conclusions deduced from x-ray powder diffraction which excluded the possible $CeNiSi_2$-type structure for these compounds.[8] Comparison between the observed and calculated intensities of the nuclear peaks for each compound are given in Tables III and IV as well as the y values and the reliability factors.

B. Magnetic structure determination

1. PrFeSi₂

Neutron-diffraction patterns recorded at 38 and 1.5 K are shown on Fig. 2. The neutron-diffraction diagram recorded at $T=38$ K is characteristic of only the nuclear scattering. The data obtained at 1.5 K show only an increase in the intensity of the nuclear reflection [except for (020) and (040) peaks], indicating the occurrence of ferromagnetic ordering. The absence of magnetic contributions to the $(0k0)$ reflections shows that the moments are aligned along the b axis. Taking into account the magnetic form factor of Pr^{3+}(11), the value of the magnetic moment on the Pr atom, at 1.5 K, is found to be $2.58(1)\mu_B$. This value is smaller than the one expected for the Pr^{3+} free ion, (i.e., $gJ=3.2\mu_B$). No localized magnetic moment on the Fe atoms was detected, within the accuracy of the neutron powder-diffraction experiment. Table III gives the calculated and observed intensities together with the adjustable parameters (y,μ_{Pr}). The temperature dependence of the magnetic intensities recorded step by step between room temperature and 1.5 K gives a Pr sublattice ordering temperature $T_c=26\pm2$ K in fair agreement with the bulk magnetic measurements (Table I).

The magnetic structure is shown in Fig. 3. It corresponds to a stacking of (010) ferromagnetic sheets, with

TABLE II. RFeSi₂. Atomic positions (space group: *Cmcm*).

R	4(c)	0	~0.105	$\frac{1}{4}$	Si_1	4(c)	0	0.455	$\frac{1}{4}$
Fe	4(c)	0	~0.750	$\frac{1}{4}$	Si_2	4(c)	0	0.316	$\frac{1}{4}$

TABLE III. $PrFeSi_2$. Calculated and observed intensities, y atomic positions, magnetic moments, and reliability factors at 38 and 1.5 K.

	38 K		1.5 K	
	$y_{Pr}=0.1044(6)$ $y_{Fe}=0.7509(4)$	$y_{Si(1)}=0.4646(7)$ $y_{Si(2)}=0.3195(8)$	$y_{Pr}=0.1039(1)$ $y_{Fe}=0.7507(1)$	$y_{Si(1)}=0.4642(2)$ $y_{Si(2)}=0.3200(2)$
hkl	I_0	I_c	I_0	I_c
020	38.84	39.36	39.48	39.28
040	41.38	41.90	41.40	41.61
110	8.56	7.22	46.62	46.33
021	~0.00	0.88	48.86	49.79
130	~0.00	1.90	7.45	7.51
041	16.70	15.85	23.89	23.73
060 111	60.85	61.06	105.36	105.55
150	129.50	127.60	152.00	151.62
131	666.90	662.00	755.00	757.09
061	141.00	133.90	140.00	138.91
151	224.85	225.10	226.18	226.14
080	35.66	35.96	35.44	34.97
200	358.00	359.61	390.00	388.21
220 002	440.00	435.93	470.00	466.93
022	77.59	77.19	80.09	80.26
081	113.44	113.25	128.03	127.56
171	516.23	515.89	561.35	559.36
μ_{Pr} (μ_B)			2.58(1) ‖b	
R_w	3.7%		0.7%	

moments perpendicular to the sheets.

2. *$NdFeSi_2$*

Neutron-diffraction patterns recorded at 16, 4.2, and 1.5 K are shown in Fig. 4. The neutron-diffraction diagram at 16 K is characteristic of only the nuclear scattering. At 4.2 and 1.5 K, the unit cell is refined with lattice constants $a=4.072(1)$ Å, $b=16.896(4)$ Å, and $c=3.996(1)$ Å. The Bragg-angle values of a series of superlattice lines are consistent with an incommensurate magnetic ordering. They may be indexed as satellites of the nuclear peaks by considering the propagating vector $\mathbf{q}=(0,\tau,0)$, with $\tau=0.591(5)$ (Table IV). The absence of the $(010)^{\pm}$ peaks demonstrates that the moments align themselves along the b axis. Nuclear peaks do not show any magnetic contribution to their intensities so that any ferromagnetic component should be excluded. Therefore, the magnetic structure is of a modulated amplitude of the longitudinal-spin-wave-type (LSW) with the b axis as the direction of both the modulation and the magnetic moments.

Since the magnetic contributions are observed on the satellites $(hkl)^{\pm}$ with $h+k=2n$, this implies that the phase difference between magnetic moments deduced from each other by a C translation is given by $2\pi\tau$. In

TABLE IV. $NdFeSi_2$. Calculated and observed intensities, y atomic positions, and reliability factor at 16 K.

	$y_{Nd}=0.1028(6)$ $y_{Fe}=0.7527(7)$	$y_{Si(1)}=0.4614(12)$ $y_{Si(2)}=0.3232(11)$
hkl	I_0	I_c
020	7.27	7.64
040	3.47	3.49
110	~0.00	0.07
021	2.47	1.30
130	1.76	2.01
041	9.50	10.84
060 111	24.43	22.89
150	72.48	50.11
131	265.60	269.60
061	56.80	53.60
151	65.70	63.14
080	10.89	11.61
200	130.84	124.97
220 002	162.68	139.89
022	13.67	14.98
081	51.15	51.51
171	78.52	79.15
R_w	5.2%	

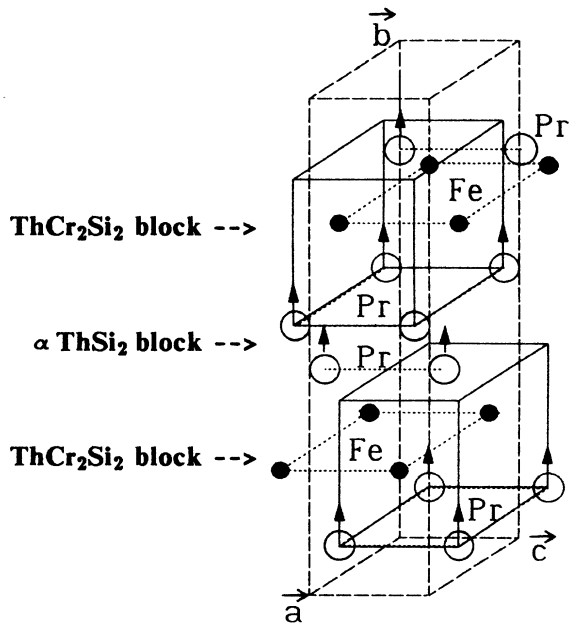

FIG. 3. Magnetic structure of $PrFeSi_2$.

the $TbFeSi_2$-type structure there are four Nd atoms per unit cell which can be divided in two sets of Nd atoms (not related by the C translation) (Table V).

Therefore, a phase difference $\Delta\phi$ must be introduced between the two sublattices. In the refinements, we have considered the two Nd sublattices as sharing the same magnetic moment amplitude. Under this reasonable assumption, the magnetic structure consists in two families of ferromagnetic (010) planes, where spins, perpendicular to the planes, are modulated along the b direction (Fig. 5).

TABLE V. $NdFeSi_2$. Equivalent atomic positions of the two sets of Nd atoms.

Nd(1)	0	y	$\frac{1}{4}$
	$\frac{1}{2}$	$\frac{1}{2}+y$	$\frac{1}{4}$
Nd(2)	0	$-y$	$\frac{3}{4}$
	$\frac{1}{2}$	$\frac{1}{2}-y$	$\frac{3}{4}$

The magnitude of the magnetic moment, $\Delta\phi$, and the y values were determined from a least-squares procedure.[10] In the refinement, the magnetic intensities were calculated taking into account the magnetic form factor of Nd^{3+} ion,[11] and assuming that iron is nonmagnetic. The best fit leads to $\mu_0=2.55(16)\mu_B$ and $\mu_0=3.17(13)\mu_B$ for the maximum amplitude of a sine-modulated moment at 4.2 and 1.5 K, respectively. The determined value of the phase difference, $\Delta\phi$, between the two Nd-sublattice waves is close to $5\pi/6$ and temperature independent. Table VI gives the calculated and observed intensities as well as the adjustable parameters $[y,\mu_0(\text{Nd}),\Delta\phi]$. The magnetic structure is shown in Fig. 5. Temperature dependence of the intensities of the magnetic reflections yields a Néel temperature of $T_N=6.0(1)$ K in good agreement with the magnetization data (Table I).

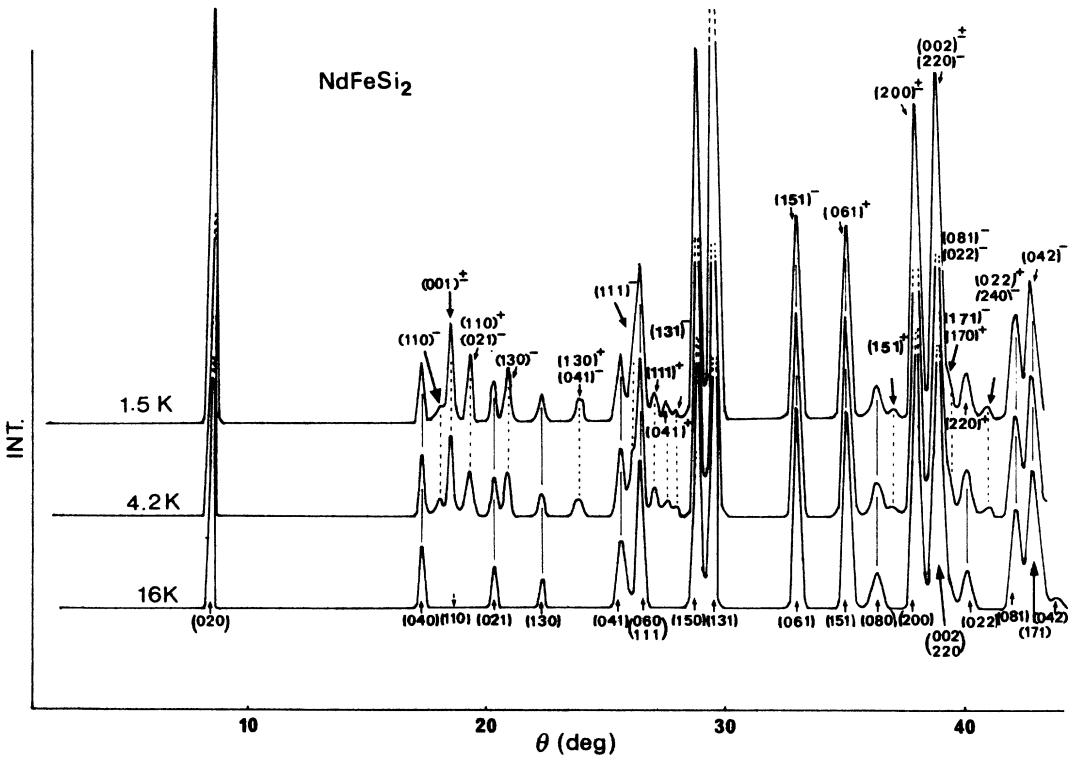

FIG. 4. Neutron-diffraction patterns of $NdFeSi_2$ at 16, 4.2, and 1.5 K.

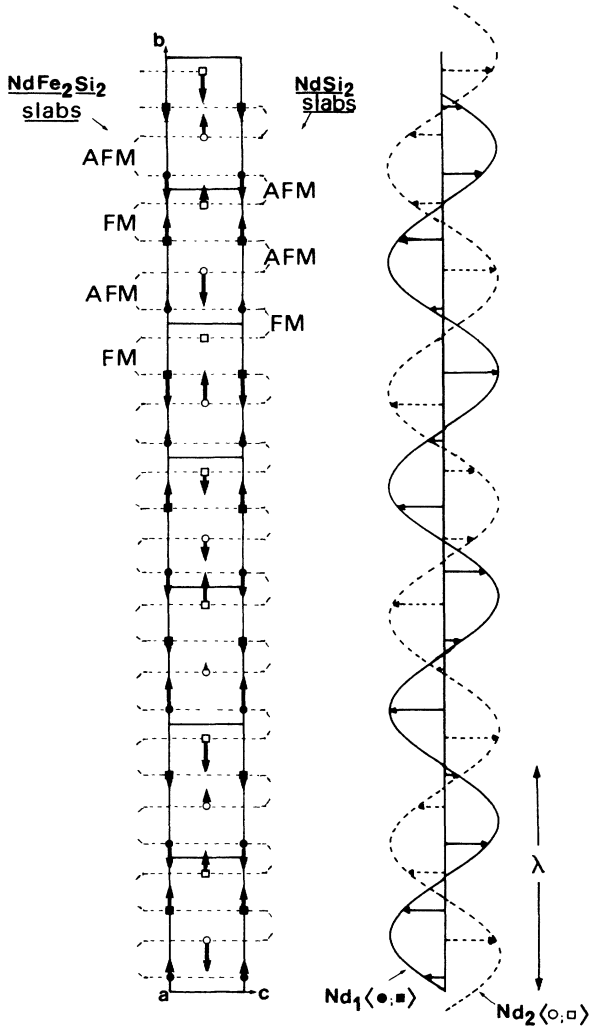

FIG. 5. Magnetic structure of $NdFeSi_2$ deduced from neutron diffraction experiment.

These results obtained from a powder sample do not allow us to choose between a *sine-modulated* structure with a maximum value of the magnetic moment $m_0 = 3.2\mu_B$ and one with a square-wave with a constant moment. Both structures generate the sequence of peaks $(h, k \pm \tau, 1)$ but the square-wave structure would also generate higher odd harmonics, e.g., $(h, k \pm 3\ \tau, 1)$. The third harmonics are not observed in our patterns; either they do not really exist or cannot be observed because they may be too weak. If calculated on the basis of the first harmonic intensities, they are expected to be very small, within the experimental resolution.

On the other hand, the strength of the calculated moment at 4.2 K for the sine-modulated moment is close to the theoretical value while the square modulated model would lead to a magnetic moment $m_0 = 2.52(20)\mu_B$, close to the value observed in $PrFeSi_2$. Furthermore, Nd^{3+} being a Kramers ion, all its crystal-field levels are magnetic in $NdFeSi_2$ and the sine-modulated structure cannot be stable down to 0 K (Refs. 12 and 13) but should rather transform (i) either into a commensurate AF structure with constant moment (which is not valid here) or (ii) to an antiphase structure (square-type) without a defined transition. Similar magnetic behaviors have been already encountered in the closely related $ThCr_2Si_2$-type structure compounds such as UM_2X_2 (M=Ni,Pd;X=Si,Ge) (Refs. 14 and 15), PrM_2Ge_2 (M=Fe,Co) (Refs. 16–18), and also in the whole RNi_2Si_2 series (Refs. 19–21) and more recently in $TmCu_2Si_2$ (Ref. 22) and $CeRh_2Ge_2$.[23]

However, in the case of $NdFeSi_2$, this ambiguity is fairly solved by ^{57}Fe Mössbauer spectroscopy.

IV. ^{57}FE MÖSSBAUER SPECTROSCOPY

A. Mössbauer data in the paramagnetic state

The Mössbauer spectra of $PrFeSi_2$ and $NdFeSi_2$ recorded at 295 and 77 K are well represented by a single quadrupole-split doublet [Table VII, Fig. 6(a)]. Table VII shows that the quadrupole splitting $E_Q = |\frac{1}{2}e^2q_zQ(1+\eta^2/3)^{1/2}|$ increases slightly by lowering the temperature. The isomer shift values of about 0.22 mm/s at 295 K (relative to iron metal) compare to those observed in other iron-silicon compounds in which Fe is nonmagnetic (e.g., RFe_2Si_2).[24] The occurrence of a small positive isomer shift (i.e., lower electron density) is tentatively attributed to the partial filling of the iron d bands by charge transfer from the silicon atoms.[24] The quadrupole interactions (0.25–0.30 mm/s) are similar to those found in RFe_2Si_2 compounds; they are primarily related to the distortion of the iron nearest neighbors Si tetrahedron (Fig. 1).

B. Mössbauer results in the ordered state of $PrFeSi_2$

In a previous work we demonstrated that $PrFeSi_2$ orders ferromagnetically at $T_c = 26$ K (Ref. 8) and the neutron data (Sec. III) showed that the Pr moments align along the b axis. No localized moment was detected on the iron atom.

The Mössbauer spectrum of $PrFeSi_2$ taken at 4.2 K [Fig. 6(d)], i.e., in the ordered state, clearly provide evidence for the presence of an internal field at the Fe nucleus due to the ordering of the Pr sublattice. The spectrum was analyzed by diagonalizing the full nuclear Hamiltonian assuming a single magnetic site. The fitting routine provides the hyperfine field H_{hf}, the isomer shift δ_{is}, the quadrupole coupling constant e^2q_zQ, the asymmetry parameter η, and the polar angles (Θ,ϕ) which define the direction of H_{hf} in the electric-field-gradient (EFG) tensor principal-axes system. It is well known[25,26] that only H_{hf}, δ_{is}, and EQ are determined without ambiguity from the spectrum of a powder sample (Table VIII). When η is large, as here, it turns out impossible to deduce the sign of e^2q_zQ; thus, two sets of solutions with positive and negative e^2q_zQ are given in Table VIII. Furthermore, equally good quality fits (χ^2) were obtained with range of values for e^2q_zQ, Θ, ϕ, and η. Inside these ranges the parameters are strongly correlated, e.g., a given η value correspond to a well-defined couple of polar angles Θ, ϕ (Table VIII).

TABLE VI. $NdFeSi_2$. Calculated and observed intensites, y atomic positions, magnetic moments, and reliability factors at 4.2 and 1.5 K.

	4.2 K		1.5 K	
	$y_{Nd}=0.1035(9)$	$y_{Si(1)}=0.461(2)$	$y_{Nd}=0.1043(9)$	$y_{Si(1)}=0.464(2)$
	$y_{Fe}=0.7503(9)$	$y_{Si(2)}=0.319(2)$	$y_{Fe}=0.7502(9)$	$y_{Si(2)}=0.319(2)$
hkl	I_0	I_c	I_0	I_c
020	21.96	23.55	21.96	23.23
040	10.28	11.68	8.92	12.27
110^-	1.66	1.69	3.25	2.71
001^{+-} 110	13.95	11.41	19.47	17.43
110^+ 021^-	9.16	9.77	14.92	14.76
021	8.57	5.35	7.52	6.09
130^-	10.40	8.97	11.85	13.68
130	4.90	4.37	5.90	5.38
041^- 130^+	5.35	7.66	8.06	11.89
041	28.41	24.45	30.10	24.40
111^- 060	90.65	88.31	108.85	90.48
111 150^-				
111^+	8.91	7.88	14.48	12.06
041^+	3.30	4.88	7.20	7.53
131^-	0.75	0.23	1.49	0.49
150	183.52	198.45	202.69	179.43
131	729.40	748.82	722.31	725.92
061 151^-	168.30	166.37	171.36	172.21
151 061^+	176.15	171.35	186.95	184.55
080	24.44	31.65	44.12	38.97
151^+	3.70	9.49	13.88	14.54
200 200^{+-} 002 220 220^-	370.50	362.44	361.31	359.16
002^{+-} 081^- 022^- 008 022	505.23	422.97	419.40	427.28
220^+ 170^+ 171^-	51.13	59.16	69.40	65.00
022^+ 240^- 081	13.55	13.49	19.58	20.35
171 240 042^-	405.15	413.36	389.39	417.66
042 221^-			53.10	58.62
201^- 112^+ 112 190^-				

TABLE VI. (*Continued*).

	4.2 K		1.5 K	
	$y_{Nd}=0.1035(9)$	$y_{Si(1)}=0.461(2)$	$y_{Nd}=0.1043(9)$	$y_{Si(1)}=0.464(2)$
	$y_{Fe}=0.7503(9)$	$y_{Si(2)}=0.319(2)$	$y_{Fe}=0.7502(9)$	$y_{Si(2)}=0.319(2)$
hkl	I_0	I_c	I_0	I_c
112^-			34.11	35.86
221				
240^+				
μ_0(Nd)	sine modulated		sine modulated	
(μ_B)	2.55(16)		3.17(13)	
	$\|\|\mathbf{b}$		$\|\|\mathbf{b}$	
	$\Delta\phi=149(10)°$		$\Delta\phi=149(10)°$	
R_w	6.4%		4.1%	

The Mössbauer results in the ordered state of $PrFeSi_2$ deserve two comments. The first point concerns the origin of the hyperfine field on Fe nuclei. In the absence of local moments on Fe, the hyperfine field may be induced by conduction electron-spin polarization via the Rudderman-Kittel-Kasuya-Yosida (RKKY) mechanism. Such is the case, e.g., for the RFe_2Si_2 series[24] where fields of the same order of magnitude as in $PrFeSi_2$ have been measured. The possibility of a hyperfine field of dipolar origin is ruled out: In $PrFeSi_2$, a lattice sum over a sphere of 45 Å yields $H_{dip}=2.2$ kOe (Ref. 8), i.e., an order of magnitude smaller than the observed field of 21.6 kOe.

The second point concerns the value of the polar angle Θ. As the point symmetry of the iron site is *mm*, the principal axes system of the EFG tensor coincides with the crystallographic axes. However, it is not possible to know *a priori* which axis is the *z* axis. Therefore, since the Pr moments are along the *b* axis the angle Θ is expected to be either $\Theta=0°$ or $\Theta=90°$. This implies that the hyperfine field (or the exchange interaction) is assumed to be isotropic, i.e., the RKKY interaction is mediated by *s*-conduction electrons. The small discrepancy between the experimental Θ values with those expected under the assumption of isotropic exchange suggests the occurrence of orbital polarization of the conduction band (of partially *d* character)[27,28] which gives rise to an anisotropic transferred hyperfine field.[29] The second argument which may support our assumption is provided by the comparison of the hyperfine fields on Fe in $PrFeSi_2$ and $NdFeSi_2$ (see below) which evidences strong departure from the simple RKKY systematics, i.e., $H_{hf} \propto (g_J-1)J$.[27]

C. Mössbauer results in the ordered state of $NdFeSi_2$

As shown previously $NdFeSi_2$ orders antiferromagnetically at 6.5 K (Ref. 8) with a complex modulated spin structure. It was concluded from the neutron-diffraction work that some ambiguities remain concerning the actual nature of the magnetic structure, i.e., sine versus square modulation. To answer this question we performed ^{57}Fe Mössbauer measurements on $NdFeSi_2$ at various temperatures between 4.2 and 1.6 K [Figs. 6(b) and 6(c)]. A close examination of the data shows that a shoulder develops at the right flank of the spectra when decreasing the temperature. This observation already suggests a progressive change of the magnetic structure by lowering the temperature. To analyze our Mössbauer data we assumed that the transferred fields experienced by the Fe atoms are only due to the two neighboring Nd planes. Defining the magnetic moments of the two neighboring planes (lower and upper planes) of an iron atom as μ_{R_-} and μ_{R_+} we can defined H_{hf} as given by

$$H_{hf}=A(\mu_{R_-}+\mu_{R_+}) . \quad (1)$$

TABLE VII. Hyperfine interaction parameters for ^{57}Fe in $PrFeSi_2$ and $NdFeSi_2$ at 295 and 77 K. δ_{IS}: isomer shift relative to iron metal at room temperature; E_Q: quadrupole splitting; W: full linewidth at half maximum.

	T (K)	δ_{IS} (mm/s)	E_Q (mm/s)	W (mm/s)
$PrFeSi_2$	295	0.220(2)	0.247(1)	0.296(2)
	77	0.327(2)	0.292(1)	0.289(2)
$NdFeSi_2$	295	0.217(2)	0.253(1)	0.285(2)
	77	0.327(2)	0.300(1)	0.277(2)

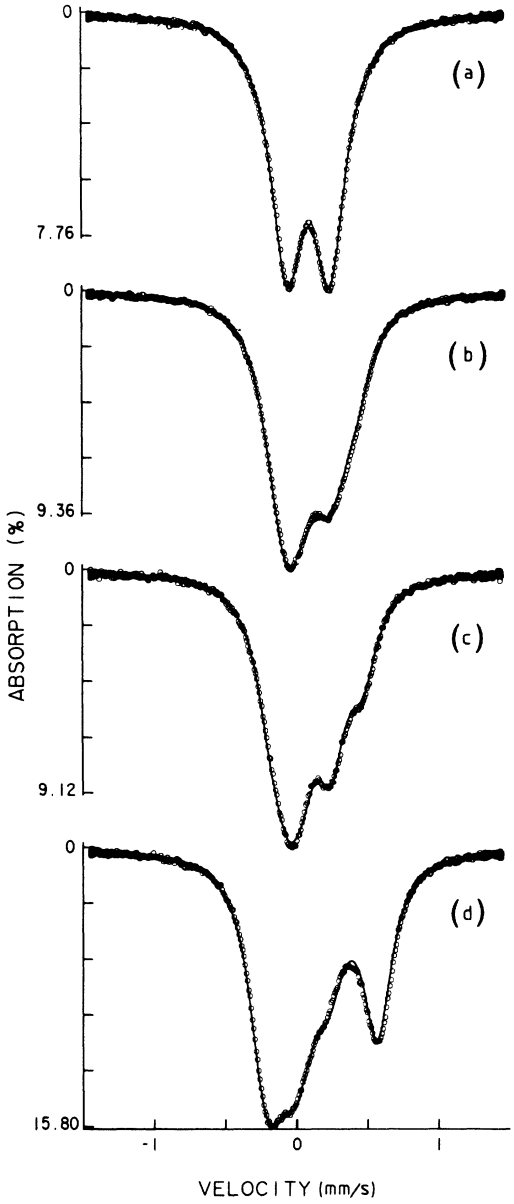

FIG. 6. ^{57}Fe Mössbauer spectra of $PrFeSi_2$ and $NdFeSi_2$ at various temperatures: $NdFeSi_2$ at 77 K (a), 4.2 K (b), and 1.6 K (c); $PrFeSi_2$ at 4.2 K (d).

For a sine-modulated structure (Fig. 5)

$$\mu_{R_-} = \mu_0 \sin 2\pi\tau y \ ,$$

TABLE VIII. Hyperfine interaction parameters for ^{57}Fe in $PrFeSi_2$ at 4.2 K (see text). δ_{IS}: isomer shift relative to iron metal at room temperature.

H_{hf} (kOe)	E_Q (mm/s)	δ_{IS} (mm/s)	W (mm/s)
21.6(5)	0.269(5)	0.333(3)	0.242(3)
e^2q_zQ (mm/s)	Θ (deg)	ϕ (deg)	η
(−0.476)–(0.466)	78.7–80.2	90–78	0.92–1
0.467–0.489	15–21	42–0	1–0.8

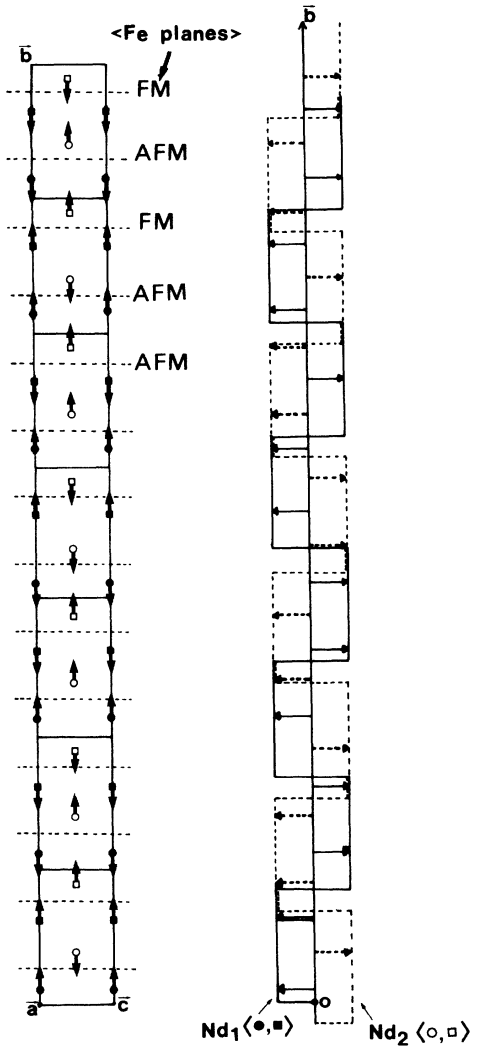

FIG. 7. Magnetic structure of $NdFeSi_2$ at 1.6 K deduced from ^{57}Fe Mössbauer spectroscopy.

and (2)

$$\mu_{R_+} = \mu_0 \sin(2\pi\tau y + 2\pi\tau d - \Delta\phi) \ ,$$

where μ_0 is the amplitude of the sine-modulated magnetic moment, τ is the propagation vector, y is the real-space

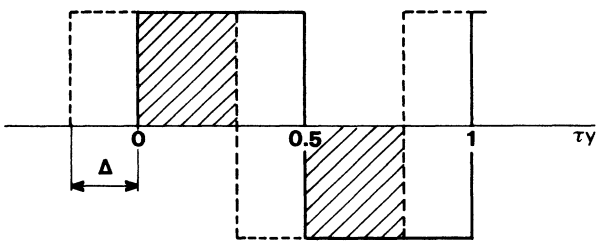

FIG. 8. Scheme of the square-modulation of the Nd moments of the two neighboring planes of an iron atom. The hatched area represents the fraction of the iron atoms which experiences a magnetic field (see text).

TABLE IX. Hyperfine interaction parameters for ^{57}Fe in $NdFeSi_2$ at 1.6 K. The iron site with zero field is assumed to have the same isomer shift and quadrupole splitting as the iron site of population p^+ experiencing an hyperfine magnetic field. δ_{IS}: isomer shift relative to iron metal at room temperature.

H_{hf} (kOe)	E_Q (mm/s)	δ_{IS} (mm/s)	p^+ (%)
14.95(6)	0.300[a]	0.330(3)	58.8(6)
e^2q_zQ (mm/s)	Θ (deg)	ϕ (deg)	η
(−0.578)–(−0.555)	80.6–86.6	90–65	0.48–0.71

[a]Fixed value.

distance of the μ_{R_-} planes given by $y=y_0b+(n-1)b/2$ where n is an integer (1 to ∞), y_0 is the positional parameter of the Nd atoms in the unit cell [$y_0=0.1043(9)$ at 1.5 K] and b the lattice parameter, d is the distance between two neighboring rare-earth planes, and $\Delta\phi$ is the phase shift between the modulated μ_{R_-} and μ_{R_+} moments.

For a square-modulated structure (Fig. 7), we expect the occurrence of two iron sites: one site with zero field (p^-) and another site (p^+) experiencing a field H_{hf} of $2A\mu_0$ (Fig. 8). The population of the two sites being given by the relations

$$p^+=|1-2\Delta|, p^-=1-p^+$$

and (3)

$$\Delta=\tau/2-2\tau y-\Delta\phi/2\pi ,$$

where $\Delta\phi$ is in radians and y is in unit of lattice parameter b (Fig. 8).

The 1.6 K spectrum which shows more structure was analyzed using either the square or the sine-modulated spin structure model. The number of free parameters was reduced by fixing the linewidth to 0.245 mm/s (as found for $PrFeSi_2$ at 4.2 K) and the quadrupole interaction EQ to the value obtained at 77 K, i.e., 0.30 mm/s. It was found that only the square-modulated model can reproduce the experimental data at 1.6 K. The results are given in Table IX.

From the experimentally determined p^+ value of 0.588(6) and taking $y=0.1043(9)$ and $\tau=0.591(5)$ as determined from the neutron data, we calculated from Eq. (3) the phase shift $\Delta\phi$ to be $136\pm8°$. This value compares well with the value estimated from the neutron experiments ($\Delta\phi=149\pm10°$).

As already mentioned a progressive change of the spectral shape appears when raising the temperature from 1.6 to 4.2 K. From this behavior it may be anticipated that the magnetic structure, square-modulated at low temperature, evolves towards sine-modulated at higher temperature.

The analysis of the 4.2 K data indicates however that the sine-modulated region is not yet reached. Thus, we analyzed the data in the temperature range $1.6<T\leq4.2$ K in the framework of a partial squaring of the modulated magnetic moments. The magnetic fields acting at the iron nucleus are then given by the relation:

$$H_{hf}=\Sigma H_m[\sin(m2\pi\tau y)+\sin(m2\pi\tau y+m2\pi\tau d-\Delta\phi)] , \quad (4)$$

where $m=1,3,5,\ldots$. (For a complete squaring $H_m=H_1/m$.)

Owing to the poor spectral resolution Eq. (4) was truncated to the third harmonic and the computation of the spectral shape was performed by considering 100 lattice points [i.e., the spectral shape is the convolution of 100 subspectra corresponding to $y=y_0b+(n-1)b/2$ with $n=1$ to 100; the spectral shape was found to be stable when $n\geq50$]. The results are summarized in Table X.

It should be noticed that the influence of higher harmonics ($m>3$) may safely be neglected only close to the region (4.2 K) where sine-modulation occurs. This is certainly no longer true at 3.0 K which is too close to the square-modulation region. Nevertheless, Table X shows that the third harmonic develops when decreasing the temperature thus confirming the progressive squaring of the modulation of the Nd magnetic moments.

For an isostructural series it is generally assumed that the transferred field should be, in a first approximation, proportional to the spin $S=(g_J-1)J$ of the rare-earth atoms and to the weighted vector sum of the magnetic moments in the vicinity of the Fe atoms. Considering, as assumed above, that the polarization of the conduction electrons is mainly due to the two neighboring R planes of an iron atom, the transferred fields observed in $PrFeSi_2$ and in the square-modulated phase of $NdFeSi_2$ (ferromagnetic coupling of the two planes) is given by

$$H_{hf}=2H_s(g_J-1)J(\mu_{ord}/\mu_{FI}) , \quad (5)$$

TABLE X. Magnetic hyperfine interaction parameters for ^{57}Fe in $NdFeSi_2$ as a function of the temperature. H_1 and H_3 are defined in Eq. (4); H_{av} is the average field and σ the standard deviation. The phase shift $\Delta\phi$ was assumed to be temperature independent and equal to 136° (see text).

	T (K)	H_1 (kOe)	H_3 (kOe)	H_{av} (kOe)	σ (kOe)
partial	4.2	7.75(3)	1.38(5)	7.61	4.67
squaring	3.6	8.47(4)	1.91(6)	8.28	5.38
	3.0	9.16(7)	2.0(1)	8.95	5.78
			H_{hf} (kOe)		
squaring	2.0		14.66(7) and 0		
	1.6		14.95(6) and 0		

where μ_{ord} and μ_{FI} are the magnetic moments of the R atoms in the ordered state and in the free ion, respectively. H_s is the field produced by unit spin. Taking $\mu_{ord}(Pr)=2.57\mu_B$ and $\mu_{ord}(Nd)=2.52\mu_B$ (see neutron data) we deduce the magnitude of H_s to be $|16.8|$ kOe and $|7.9|$ kOe for $PrFeSi_2$ and $NdFeSi_2$, respectively.

The strong deviation of H_{hf} from Eq. (5) (H_s should be a constant for isostructural compounds with similar band structures) may be explained if we add significant orbital contributions to the transferred field.[27]

V. DISCUSSION

In the introduction we have emphasized the straight relationship between the $ThCr_2Si_2$, α-$ThSi_2$ and $TbFeSi_2$-type structures: $TbFeSi_2$ structure could be described as isolated $ThCr_2Si_2$-type blocks (including Fe planes) connecting via $ThSi_2$ slabs.

As in the corresponding RFe_2Si_2 compounds,[5] we observed that iron is nonmagnetic.

The $NdFe_2Si_2$ and $NdFeSi_2$ magnetic structures at 1.5 K are shown on Fig. 9. The great similarity between these two compounds appears clearly. Thus, the long-range modulated magnetic structure of $NdFeSi_2$ results in $NdFe_2Si_2$ blocks where internal couplings are either negative or positive as observed in $NdFe_2Si_2$ compound.

The $NdFe_2Si_2$ magnetic structure is frustrated since the I translation (centering) corresponds to alternate positive and negative magnetic couplings. An antiferromagnetic next-nearest-neighbor interaction ($d_3 \sim 10$ Å) much stronger than those acting between nearest layers ($d_1 \sim 5.7$ Å) was invoked as responsible for such a coupling sequence (Fig. 10).[6] In $NdFeSi_2$, such a long distance interaction could be invoked [$d_4 \sim 8.73$ Å, (Fig. 10)] and possibly explains the similar magnetic behavior observed in this compound. Indeed, the noncommensurate magnetic order observed in $NdFeSi_2$, probably results from the competition between negative, Nd(1)-Nd(2)(d_1), Nd(1)-Nd(3)(d_3), and Nd(1)-Nd(2)(d_4) interactions (cf. Fig. 10). These long range magnetic structures are probably stabilized, in both compounds, by dominant RKKY-type interactions.

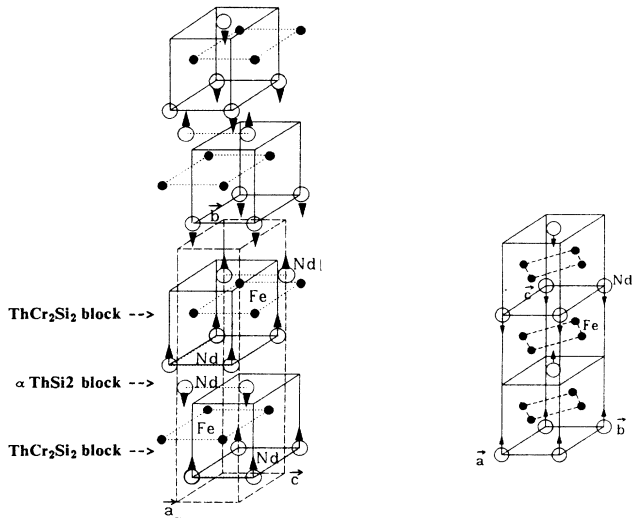

FIG. 9. Magnetic structures of (a) $NdFeSi_2$ and (b) $NdFe_2Si_2$ (4).

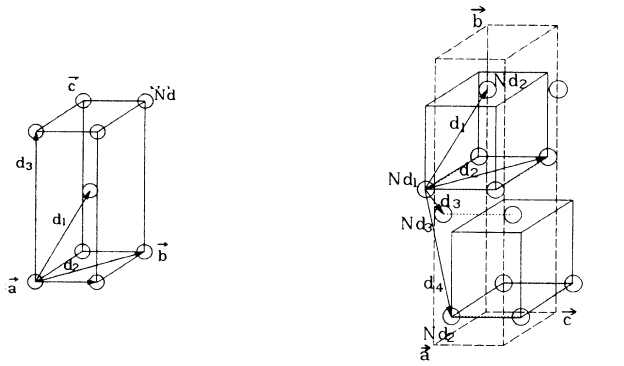

FIG. 10. R-R interatomic distances in $TbFeSi_2$ and $ThCr_2Si_2$-type structures.

It may be noticed that the easy axis is also the same in the two parent compounds (reference to the stacking sequence of metal planes). The different values of the moments observed for the two compounds ($3.2\mu_B$ in $NdFe_2Si_2$ against $2.5\mu_B$ in $NdFeSi_2$) probably results from different CEF states due to the different local symmetry of Nd in each compound ($4/m$ in $NdFe_2Si_2$, mm in $NdFeSi_2$). Furthermore, Mössbauer spectroscopy confirms the similarity of the magnetic behavior of the two compounds. Taking into account the different values of the Nd magnetic moments, the value of the transferred hyperfine field, observed in each compound, shows that the inserted iron planes in the $ThCr_2Si_2$-type block of $NdFeSi_2$ and $NdFe_2Si_2$ (Ref. 24) have similar magnetic neighboring of Nd atoms.

On the other hand, the analysis of a/c ratio determined for a large number of RT_2X_2 intermetallic compounds[30,31] indicates that for $a/c > 1/\sqrt{6}(=0.4082)$ an oscillatory magnetic ordering scheme appears. Calling d_1 the interplanar R-R distance and d_2 the intraplanar R-R distance (along [110])(Fig. 10), this critical ratio corresponds to $d_1=d_2$ (i.e., $a/c > 0.4082$ is equivalent to $d_2 > d_1$). A similar criterion can be elaborated in the $TbFeSi_2$ type, the considered distances being then

$$d_1=\left[\frac{a^2}{4}+(\tfrac{1}{2}-2y_R)^2b^2+\frac{c^2}{4}\right]^{1/2}$$

and

$$d_2=(a^2+c^2)^{1/2} \text{ (Fig. 10)} .$$

The values of d_1 and d_2 for $NdFe_2Si_2$ and $NdFeSi_2$ are given in Table XI.

It is very interesting to note that the ratio criterion ($d_2 > d_1$) is fulfilled for the modulated magnetic structure of $NdFeSi_2$ and not for the simple collinear magnetic structure of $NdFe_2Si_2$, $a/c=0.398$ for $NdFeSi_2$.[24]

We also emphasized that the $NdSi_2$ slabs connecting

TABLE XI. Interatomic R-R interplanar (d_1) and intraplanar (d_2) distances in $NdFe_2Si_2$ ($ThCr_2Si_2$-type structure) and $NdFeSi_2$ ($TbFeSi_2$-type structure).

	d_1 (Å)	d_2 (Å)	a/c
$NdFe_2Si_2$	6.404	5.633	0.397
$NdFeSi_2$	5.696	5.705	0.409

$NdFe_2Si_2$-type blocks in $NdFeSi_2$ have internal couplings that are essentially negative; an estimation, based on the magnetic structure at 1.6 K deduced from ^{57}Fe Mössbauer spectroscopy (Fig. 8), yields to 92% of antiferromagnetically coupled slabs. This may be connected to the fact that $NdSi_2$ compound order antiferromagnetically below 11 K.[32]

Surprisingly $NdFeSi_2$ appears to be made of $NdFe_2Si_2$ and $NdSi_2$ blocks where the magnetic interactions are comparable to those found in the $NdFe_2Si_2$ and $NdSi_2$, respectively. We noticed that the ordering temperature of $NdFeSi_2$ is lower (6 K) than those of the other two compounds [i.e., 16 K for $NdFe_2Si_2$ (Ref. 6) and 11 K for $NdSi_2$ (Ref. 32)].

For the Pr series, no magnetic ordering is observed down to 4.2 K in $PrFe_2Si_2$ (Ref. 5) while $PrSi_2$ (Ref. 32) and $PrFeSi_2$ order ferromagnetically at 11 and 26 K, respectively. In the $PrFeSi_2$ magnetic structure, the $PrSi_2$ slabs are still ferromagnetic entities. The $PrFe_2Si_2$ blocks (nonmagnetic in the $ThCr_2Si_2$-type structure material) should be considered here as ferromagnetically polarized by the next-nearest interactions. Hence, the ordering temperature T_C increases from 11 K in $PrSi_2$ to 26 K in $PrFeSi_2$.

VI. CONCLUSION

The $RFeSi_2$ compounds exhibit magnetic ordering of the R sublattices at low temperatures; ferromagnetic in $PrFeSi_2$ and antiferromagnetic with a modulation of the Nd moments in $NdFeSi_2$. No local moment on the iron sublattice was detected in any of the investigated compounds. Although neutron diffraction is not sensitive to very small magnetic moments, the absence of local iron moment is supported by the behavior of the isostructural $LaFeSi_2$ and $CeFeSi_2$ compounds which were shown to be Pauli paramagnets.[8] The occurrence of a hyperfine field at the iron site in $PrFeSi_2$ and $NdFeSi_2$ is a unique consequence of the polarization of the conduction electrons by the R magnetic moments. The ambiguity concerning the actual nature of the modulated antiferromagnetic structure of $NdFeSi_2$ as deduced from the neutron data was nicely solved by a careful examination of the temperature dependence of the ^{57}Fe Mössbauer spectra of $NdFeSi_2$ in the ordered state. A progressive squaring of the sine modulation of the Nd moments was demonstrated; the squaring being complete below 3 K. The comparison of the transferred field values at the iron nuclei in $PrFeSi_2$ and $NdFeSi_2$ showing strong departure from the simple RKKY systematics suggested the occurrence of orbital contribution to the transferred field.

The study of the magnetic orderings of $PrFeSi_2$ and $NdFeSi_2$ provided useful information on the rare-earth anisotropy and exchange interactions. The stability of the collinear magnetic structures consisting in (010) ferromagnetic planes (with moments perpendicular to the planes) may be ascribed either to anisotropic exchange interactions arising from orbital polarization of the conduction electrons or to R single-ion anisotropy plus exchange interactions. The orientation of the R moments with respect to the crystal [010] axis is probably determined by the second-order crystal-field term B_2^0. Following Greedan and Rao[33] a [010] easy axis direction indicates that B_2^0 should be negative. The influence of crystal field effects may also explain the partial quenching of the R moments which are somewhat smaller than the R free-ion values.

In both studied $RFeSi_2$ compounds, the long-range magnetic ordering along the stacking axis depends on the nearest, next-nearest. . . interactions of the RKKY type. They are probably negative for R = Nd and positive for R = Pr. The magnetic structures are very similar to those found in most of the corresponding $ThCr_2Si_2$-type structure compounds in agreement with the underlined structural relationship. However, the moments values which express crystal-field effects through the local symmetry are different.

ACKNOWLEDGMENTS

Neutron diffraction data were recorded at the Institut Laue Langevin (ILL). We are grateful to J. L. Soubeyroux, responsible for the spectrometer used, for his help during the measurements. The Laboratoire de Chimie du Solide Minéral is "Unite Associée au Centre National de la Recherche Scientifique" No. 158. The Laboratoire de Science et Génie des Matériaux Métalliques is "Unite Associée au Centre National de la Recherche Scientifique" No. 159.

*On leave from Institute of Physics, Jagellonian University, Cracow, Poland.

[1]V. I. Yarovets and Yu. K. Gorelenko, Vestn. L'vovsk Univ. Ser. Khim. **23**, 20 (1981).

[2]O. I. Bodak and E. I. Gladyshevskii, Sov. Phys. Crystallogr. **14**, 859 (1970).

[3]G. Brauer and A. Mitius, Z. Anorg. Allg. Chem. **249**, 325 (1942).

[4]P. Rogl, in *Handbook on the Physics and Chemistry of Rare Earths*, edited by K. A. Gschneidner, Jr. and L. Eyring (North-Holland, Amsterdam, 1984), Vol. 7, p. 1.

[5]A. Szytula and J. Leciejewicz, in *Handbook on the Physics and*

Chemistry of Rare Earths, edited by K. A. Gschneidner, Jr. and L. Eyring (Elsevier, New York, 1989), Vol. 12, p. 133.
[6]H. Pinto and H. Shaked, Phys. Rev. B **7**, 3261 (1973).
[7]I. Felner, I. Mayer, A. Grill, and M. Schrieber, Solid State Commun. **16**, 1005 (1975).
[8]G. Venturini, B. Malaman, M. Meot-Meyer, D. Fruchart, G. Le Caer, D. Malterre, and B. Roques, Rev. Chim. Minerale **23**, 162 (1986).
[9]A. J. Freeman and J. P. Declaux, J. Magn. Magn. Mater. **12**, 11 (1979).
[10]P. Wolfers, System MXD, Library of Programs, Laboratoire de Cristallographie, Grenoble, France (unpublished).
[11]C. Stassis, H. W. Deckman, B. N. Harmon, J. P. Desclaux, and A. J. Freeman, Phys. Rev. B **15**, 369 (1977).
[12]J. Gignoux and J. C. Gomez-Sal, Phys. Lett. **50A**, 63 (1974).
[13]P. Morin, D. Schmitt, and C. Vettier, J. Phys. **46**, 39 (1985).
[14]H. Ptasiewicz-Bak, J. Leciejewicz, and A. Zygmunt, J. Phys. F **11**, 225 (1981).
[15]L. Chelmiki, J. Leciejewicz, and A. Zygmunt, J. Phys. Chem. Solids **46**, 529 (1985).
[16]H. Pinto, M. Melamud, and E. Gurewitz, Acta Crystallogr. Sect. A **35**, 533 (1979).
[17]J. Leciejewicz, A. Szytula, and A. Zygmunt, Solid State Commun. **45**(2), 149 (1982).
[18]A. Szytula, J. Leciejewicz, and H. Binczycka, Phys. Status Solidi **58**, 67 (1980).
[19]J. M. Barandanian, D. Gignoux, D. Schmitt, and J. C. Gomez-Sal, Solid State Commun. **57**(12), 941 (1986).
[20]J. M. Barandanian, D. Gignoux, D. Schmitt, J. C. Gomez-Sal, and J. Rodriguez-Fernandez, J. Magn. Magn. Mater. **69**, 61 (1987).
[21]J. M. Barandanian, D. Gignoux, D. Schmitt, J. C. Gomez-Sal, J. Rodriguez, P. Chieux, and J. Schweitzer, J. Magn. Magn. Mater. **73**, 233 (1988).
[22]Y. Allain, F. Bouree-Vigneron, A. Oles, and A. Szytula, J. Magn. Magn. Mater. **75**, 303 (1988).
[23]G. Venturini, B. Malaman, L. Pontonnier, and D. Fruchart, Solid State Commun. **67**(3), 193 (1988).
[24]A. M. Umarji, D. Niarchos, D. R. Noakes, P. J. Viccaro, G. K. Shenoy, and A. T. Aldred, J. Magn. Magn. Mater. **36**, 61 (1983).
[25]S. V Karyagin, Sov. Phys. Solid State **8**, 391 (1966).
[26]G. Le Caer, B. Malaman, G. Venturini, D. Fruchart, and B. Roques, J. Phys. F **15**, 1813 (1985).
[27]B. D. Dunlap, I. Nowik, and P. M. Levy, Phys. Rev. B **7**, 4332 (1973).
[28]Y. Berthier, R. A. B. Devine, and E. Belorizky, Phys. Rev. B **17**, 4137 (1978).
[29]A. Balabanov, I. Felner, and I. Nowik, Solid State Commun. **18**, 823 (1976).
[30]C. Godart, L. C. Gupta, and M. F. Ravet-Krill, J. Less-Common Met. **94**, 187 (1983).
[31]J. Leciejewicz and A. Szytula, J. Magn. Magn. Mater. **63-64** 190 (1987).
[32]J. Pierre, E. Siaud, and D. Frachon, J. Less-Common Met. **139**, 321 (1988).
[33]J. E. Greedan and V. U. S. Rao, J. Solid State Chem. **6**, 387 (1973).